

Sorption-enhanced reforming of tar: Influence of the preparation method of CO₂ absorbent

Huaqing Xie, Weidong Zhang, Xiangnan Zhao, Hao Chen, Qingbo Yu[†], and Qin Qin

School of Metallurgy, Northeastern University, No. 11, Lane 3, WenHua Road,
HePing District, Shenyang, 110819, Liaoning, P. R. China
(Received 11 June 2018 • accepted 28 July 2018)

Abstract—To remove tar and produce environment-friendly H₂, one of the promising routes is the sorption-enhanced steam reforming (SESR) process, in which the CO₂ sorbent is a key element. We prepared the CO₂ sorbents with Ca₁₂Al₁₄O₃₃ as carrier with various methods. Their characterizations were examined, and the sample prepared by sol-gel (SG) method showed the strongest CaO and Ca₁₂Al₁₄O₃₃ phases and the most excellent pore structure among all the samples. Then, a thermogravimetric experiment was conducted, and the results showed that the sample prepared by sol-gel (SG) method had the best CO₂ adsorption capacity and excellent long-term cyclic stability. Finally, the sorbent was used into the steam reforming experiments of tar. Under the action of the sorbent, the reforming reaction was enhanced in-situ, with the H₂ yield and concentration improved obviously, and especially, H₂ concentration can reach over 98.85%.

Keywords: Steam Reforming, Tar Removal, Hydrogen Production, CO₂ Sorbent, Ca₁₂Al₁₄O₃₃

INTRODUCTION

Tar, having extremely complex composition largely consisting of aromatic compounds, is mainly produced from gasification and retorting (such as coking) of biomass and coal. But these thermochemical conversion technologies have some main barriers for the realization of commercial-scale production, especially for biomass gasification, because tar can cause several problems, such as condensation and clogging in the downstream equipment, thus requiring to be removed in time [1-4]. Considerable approaches, including physical and thermochemical processes, have been developed for tar elimination in recent years. For the physical process (such as scrubbers and filters), it has some limits, although tar can be removed efficiently. For example, in coking industry tar was commonly removed physically from coke oven gas (COG) via ammonia solution spraying. Although the removed tar can be further processed into naphthalene, benzene and other chemical products, these benefits commonly cannot compensate for the COG cleaning cost [5]. Additionally, the temperature of hot COG is cooled from (700-900 °C) to less than 100 °C, causing huge amounts of high-quality sensible heat loss [6]. For thermochemical process, the main method is thermal cracking, but it demands extremely high operation temperature (often over 900 °C) and large energy inputs [1,7].

Steam reforming, requiring more moderate temperatures, is considered as one of the promising routes of converting tar to light fuel

gases, and could enhance the heating value of producer gas, and especially in terms of high hydrogen production spreads a desirable prospect [8-14]. Hydrogen is an environmentally friendly and high-efficiency energy, and also an important raw material used widely in the metallurgical, petrochemical, food and fertilizer industries [15]. Catalysts play an important role for hydrogen production in the reforming process, and Ni-based catalysts have been widely employed because of their effective catalytic activity for C-C bond cleavage and low cost [16,17]. Most Ni-based catalysts are supported on Al₂O₃ carrier, but are deactivated easily due to carbon deposition and sintering or loss of active Ni component, leading to low hydrogen yield [1,3,6]. Compared to Al₂O₃, mayenite (Ca₁₂Al₁₄O₃₃) as carrier has an excellent sustainability against coke formation, attributed to having a high oxygen restored property because of its special free oxygen restored structures [18]. Li et al. [10] prepared Ni/mayenite catalyst and it showed an excellent property for biomass tar (toluene as model compound) reforming with over 80% H₂ yield. Our team prepared Ni/Ca₁₂Al₁₄O₃₃ catalyst, and found it had obviously higher catalytic activity than the catalyst with Al₂O₃ as carrier in the steam reforming process of 1-methylnaphthalene (C₁₁H₁₀) as tar model compound, and also showed an excellent resistance to coke formation with the carbon conversion over 97% [4,9]. However, common steam reforming (CSR) process generally just obtained about 70 vol% H₂ in the produced gas with over 20 vol% CO₂, to limit the application of such a hydrogen-containing gas [1,4,8,9,11,15,17].

So, the sorption-enhanced steam reforming (SESR) process was put forward to obtain high-purity H₂, by in-situ separating CO₂ from the catalytic steam reforming process to shift the reaction equilibrium to the direction for high H₂ production, and it was proved to be able to enhance H₂ yield and purity efficiently in the steam reforming processes of CH₄ and bio-oil, with a final H₂ concentra-

[†]To whom correspondence should be addressed.

E-mail: yuqb@smm.neu.edu.cn

Mailing address: Room 245A, School of Metallurgy, Northeastern University, No. 11, Lane 3, Wenhua Road, Heping District, Shenyang, Liaoning, P. R. China

Copyright by The Korean Institute of Chemical Engineers.

tion over 95% [15,17,19-24]. As a key element in the SESR process, the CO₂ sorbent is mostly CaO-based one due to its high sorption capacity. However, bulk CaO usually suffers from a sharp decay in CO₂ adsorption capacity after several carbonation/calcination cycles, and it also is easily sintered at high temperature [25,26]. To improve the sorption capacity and long-term stability, the CaO synthesis doped with inert materials as structural supports raised concern. Xie et al. [27,28] prepared and then studied CaO-based sorbent doped with Ca₉Al₆O₁₈, and it showed good reactivity and stability during multiple cycles. Because of a unique cage cavity structure with well-developed pore and good mechanical strength, Ca₁₂Al₁₄O₃₃ as the inert support material of CO₂ sorbents has also been investigated, providing a stable framework inhibiting the sintering and deactivation [18,21,29]. However, in the synthesis processes of these inert support materials, some impurity phases are always produced concomitantly, so the preparation methods have significant effects on the performances of these synthetic sorbents, but the related reports were few.

We prepared CO₂ sorbents with Ca₁₂Al₁₄O₃₃ as carrier with five different methods, and used SEM, XRD and BET analyses to characterize the properties of these samples. Then, we evaluated their CO₂ adsorption capacities and cyclic stabilities in a thermogravimetric analyzer. Finally, the sorbent with the best prepared method was applied in the steam reforming process of tar, and the reforming efficiency for hydrogen production was studied by comparing with the case without CO₂ capture.

EXPERIMENTAL

1. Sorbent Preparation

CaO-based sorbents with Ca₁₂Al₁₄O₃₃ as carrier were prepared with the ratio of CaO and Ca₁₂Al₁₄O₃₃ of 3 : 1 under five different methods: solid-state-reaction method (SSR), co-precipitation (CP) method, solid-liquid mixing (SLM) method, sol-gel (SG) method and impregnation (IM) method. For SSR method, also called high-temperature roasting method, in which analytical pure CaCO₃ and γ -Al₂O₃ were mixed well and then were calcined at 900 °C for 4 h to ensure the solid state reaction between each other thorough for the formation of Ca₁₂Al₁₄O₃₃ [30]. For CP method, the mixed solutions of Ca(NO₃)₂ and Al(NO₃)₃ were titrated by ammonia to control pH value at 10.8-12.6 and subsequently stirred magnetically for 3 h. After vacuum filtration and overnight drying, the precipitate was calcined at 900 °C for 4 h [31]. For SLM method, pure CaO was added into the Al(NO₃)₂ solution with moderate isopropyl alcohol as stabilizer, and then the solution was stirred at 70 °C till becoming a paste. Thereafter, the paste was dried overnight, and then was calcined at 900 °C for 4 h [32]. For SG method, appropriate amounts of Ca(NO₃)₂·4H₂O and Al(NO₃)₂·9H₂O were dissolved in 20 wt% citric acid (CA) solution, with small amount of polyethylene glycol as surfactant, and then the solution was stirred at 70 °C for 3 h to form a transparent solution, and then was added by ethylene glycol (EG), stirred for 3 h, leading to a sol. Subsequently, the sol was placed at 90 °C for 24 h to form a gel, and then the gel was heated to 600 °C through a self-combustion process. Finally, the sample was further calcined at 900 °C for 4 h after grinding [4,33]. For IM method, the carrier of Ca₁₂Al₁₄O₃₃ was first prepared with the SG method as the above with the mole ratio of Ca(NO₃)₂·4H₂O

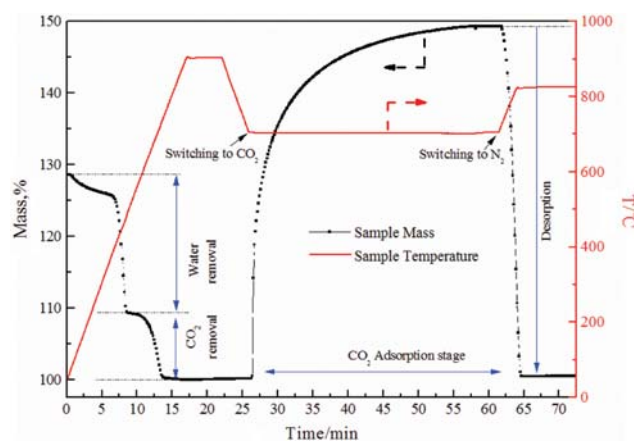


Fig. 1. The heating procedure of the thermogravimetric experiment.

and Al(NO₃)₃·9H₂O of 6 : 7, and then the carrier was mixed with the aqueous solution of Ca(NO₃)₂·4H₂O and stirred for 3 h, dried over night at 110 °C, afterwards calcined at 900 °C for 4 h.

2. Sorbent Characterization

The crystalline structures of the sorbents were characterized by X-ray diffraction (XRD, Shimadzu, XRD-7000) using Cu K α radiation operated at 30 kV and 40 mA. The morphologies of the sorbents were examined by scanning electron microscope (SEM) using a Hitachi SU-8010 microscope. Specific surface areas of the sorbents were measured with a N₂ adsorption apparatus (ASAP-2010, Micromeritics), using nitrogen physisorption and desorption isotherms at -196 °C.

3. Experimental Apparatus

The CO₂ adsorption performance of the sorbent samples was tested with a Netzsch STA409C thermogravimetric analyzer; its heating procedure is shown in Fig. 1. Before adsorbing CO₂, the samples were preprocessed by heating the furnace temperature to 900 °C with nitrogen as the inert gas to remove its own water and CO₂, which were adsorbed in the preparation and storage processes. The adsorption process was conducted at 700 °C with 50 mL/min CO₂ as the input gas. Then, the input gas was switched to N₂, and the furnace temperature was heated to 825 °C, to realize the regeneration of the sorbent samples. Next, the furnace was cooled. But for the cyclic tests, the temperature was decreased to 700 °C and the previous procedures were repeated.

The optimal sorbent was used in the experiment of catalytic steam reforming of tar, with the experimental apparatus shown in Fig. 2. The sorbent was mixed with the reforming catalyst in the same mass and packed in the stainless-steel downstream reactor. The catalyst used was Ni/Mg-Ca₁₂Al₁₄O₃₃, of which the preparation and performance were reported in the literature [9]. The tar and distilled water were pumped into the reactor drop by drop through two peristaltic pumps, with 600 mL/min nitrogen as carrier gas. For simplification of analysis, 1-methylnaphthalene (C₁₁H₁₀) was used as the tar model component in the reforming experiments, because it is decomposed into naphthalene and benzene under high temperature, and such a reaction process approaches the conversion process of the real tar [3,14]. The reforming experiments were performed at the S/C ratio (the mole ratio of the input

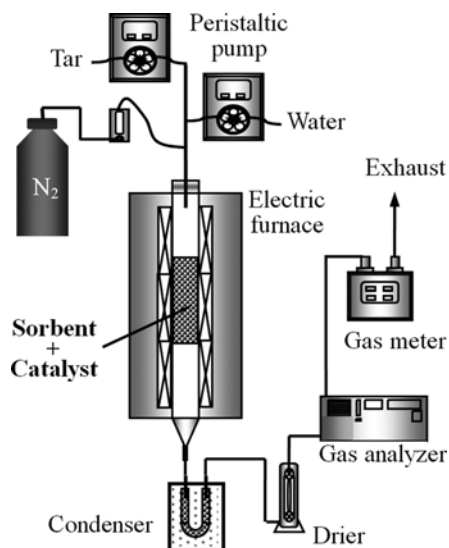


Fig. 2. The schematic illustration of experiment apparatus.

water and the carbon in the tar) of 12:1 and the WHSV (weight hourly space velocity) of 0.128 h⁻¹.

4. Data Analysis

In this paper, the CO₂ adsorption capacity is defined as the mass change after adsorption per unit mass of sorbent, as presented by Eq. (1).

$$\text{CO}_2 \text{ adsorption capacity} = \left(\frac{\text{mass of sorbent after adsorption}}{\text{mass of sorbent before adsorption}} - 1 \right) \times 100\% \quad (1)$$

In the reforming experiment, the H₂ yield (y_{H_2}) and the composition concentrations (C_x , x is H₂, CO, CO₂ or CH₄) of the reformed gas were investigated, and they were defined as Eq. (2) and Eq. (3), respectively.

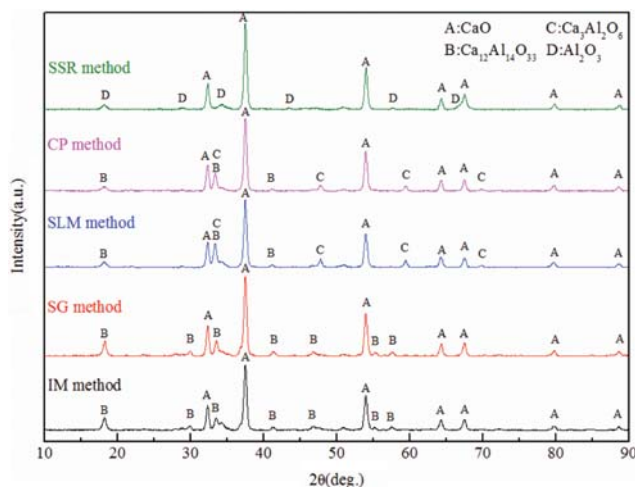


Fig. 3. XRD patterns of the sorbent samples with different preparation methods.

$$y_{H_2} = \frac{\text{moles of H}_2 \text{ in the gaseous products}}{\text{theoretical moles of H}_2 \text{ obtained}} \times 100\% \quad (2)$$

$$C_x = \frac{\text{moles of } x \text{ in the reformed gas}}{\text{total moles of the reformed gas}} \times 100\% \quad (3)$$

RESULTS AND DISCUSSION

1. Characterization

Fig. 3 illustrates the diffraction patterns of the sorbents with different preparation methods. It is clear that the characteristic peaks of CaO as the active component of sorbent were obviously detected at $2\theta = 32.32^\circ$, 37.46° , 53.97° for all the samples. For SSR method, its CaO peaks were the highest among all samples, with other crystal phases (such as Al₂O₃ and Ca₃Al₂O₆) also detected, but the phase

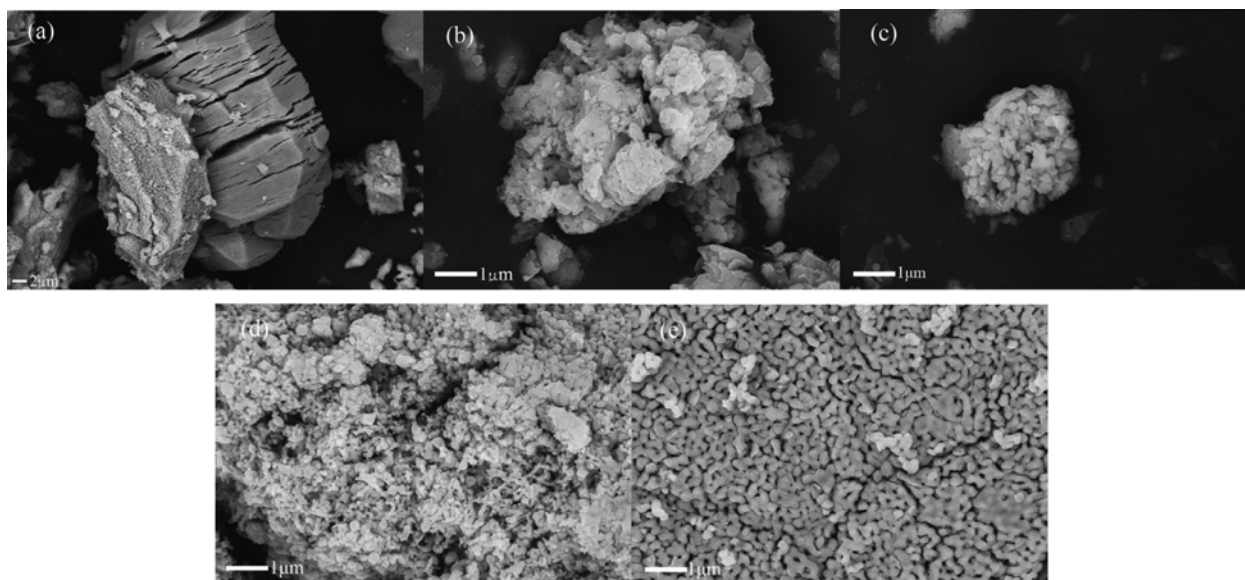


Fig. 4. SEM images of the sorbent samples with different preparation methods with a 20,000× magnification. (a) SSR, (b) CP, (c) SLM, (d) SG and (e) IM.

Table 1. The specific surface area of sorbents with different preparation methods

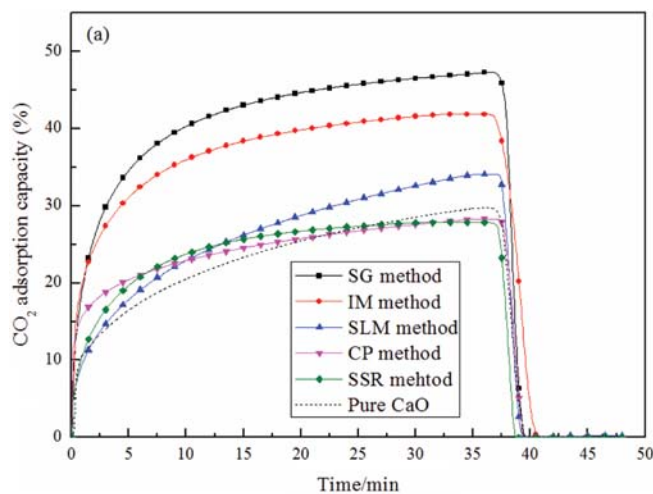
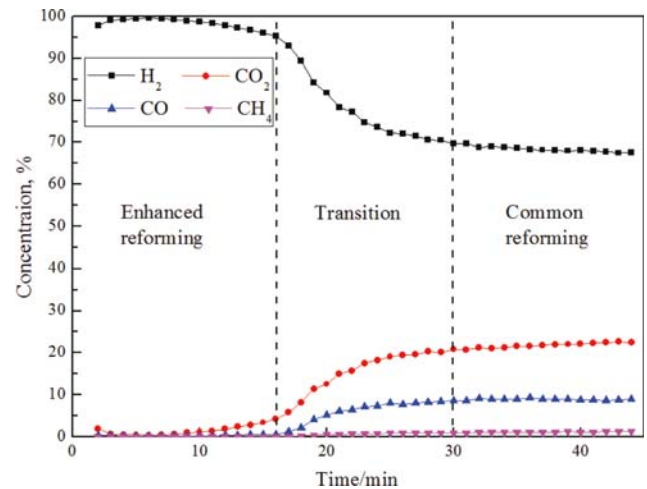
Method	SSR	CP	SLM	SG	IM
BET (m ² /g)	5.7	9.2	15.5	20.8	19.6

of Ca₁₂Al₁₄O₃₃ as the carrier of sorbent was almost not found. It indicated that solid state reactions or the ideal reactions between the precursors hardly occurred, mainly because the precursor particles could not contact highly and closely with each other. For CP and SLM method, the characteristic peaks of Ca₁₂Al₁₄O₃₃ as well as those of CaO were detected, but there were still some interference phases. For SG and IM method, they had the similar XRD patterns with the obvious characteristic peaks of CaO and Ca₁₂Al₁₄O₃₃ and no other interference phases.

The SEM images and specific surface areas of the sorbents with different preparation methods are illustrated in Fig. 4 and Table 1, respectively. For SSR method, due to no formation of the skeleton carrier, the sample had a more dense structure with the smallest specific surface area in all the samples. For CP and SLM method, the pore structures of the two samples were developed better than that of the sample prepared by SSR, attributed to the skeleton formation. For SG method, the sample exhibits much smaller sizes of the grains distributed evenly on the sorbent surface, and has the most excellent pore structure with the highest specific surface area. For IM method, it also formed a uniform structure yet with slightly bigger grain sizes, mainly because during the impregnation process the used carrier was prepared by the SG method in advance, but the impregnated carrier then underwent the second calcination, causing the grain aggregation.

2. CO₂ Adsorption Performance

Fig. 5(a) and (b) show the CO₂ adsorption capacities and cyclic stabilities of the sorbents with different preparation methods, respectively. Among all the samples, the one prepared by SG method showed the best CO₂ adsorption capacity, followed by the ones by IM method and then SLM method, which was consistent with their characterization results. For CP and SSR method, the adsorp-

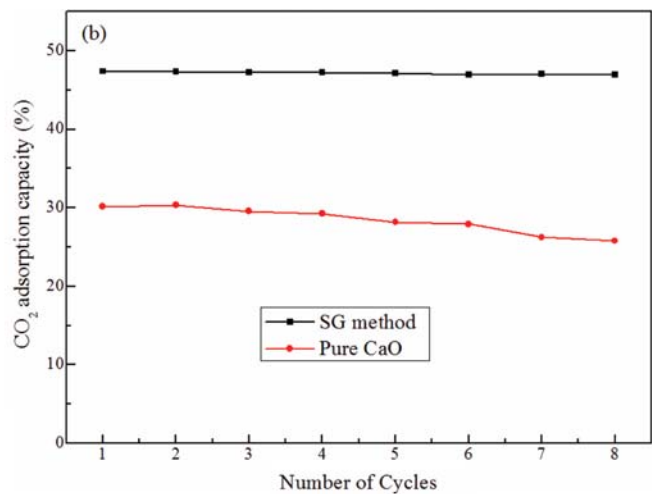
**Fig. 5. CO₂ adsorption capacities of the sorbent samples.****Fig. 6. The change curves of the product concentrations.**

tion abilities of their samples were the lowest, yet still almost equal with that of pure CaO. For the sample prepared by SG method, it also showed an excellent long-term cyclic stability with almost no change of its adsorption capacity after multiple cycles, attributed to the Ca₁₂Al₁₄O₃₃ carrier providing a stable framework inhibiting the sintering and deactivation of CaO. Contrarily, the pure CaO without any carrier support showed an obvious decreasing trend with the increase of the cycle number.

3. Application in the SESR Process

From the above, the CO₂ sorbent by SG method has the best adsorption performance among all the prepared sorbents in this paper. So, the sorbent was used into the SESR experiment of tar in the following.

Fig. 6 shows the change curves of the product concentrations in the reforming process. At the initial stage, CO₂ concentration in the reformed gas was extremely low, because CO₂ produced from the SR reaction was captured in-situ by fresh CO₂ sorbent, then displacing the equilibriums of the C_nH_m (including CH₄) steam reforming reactions (Eq. (4)) and the WGS reaction (Eq. (5)) to the



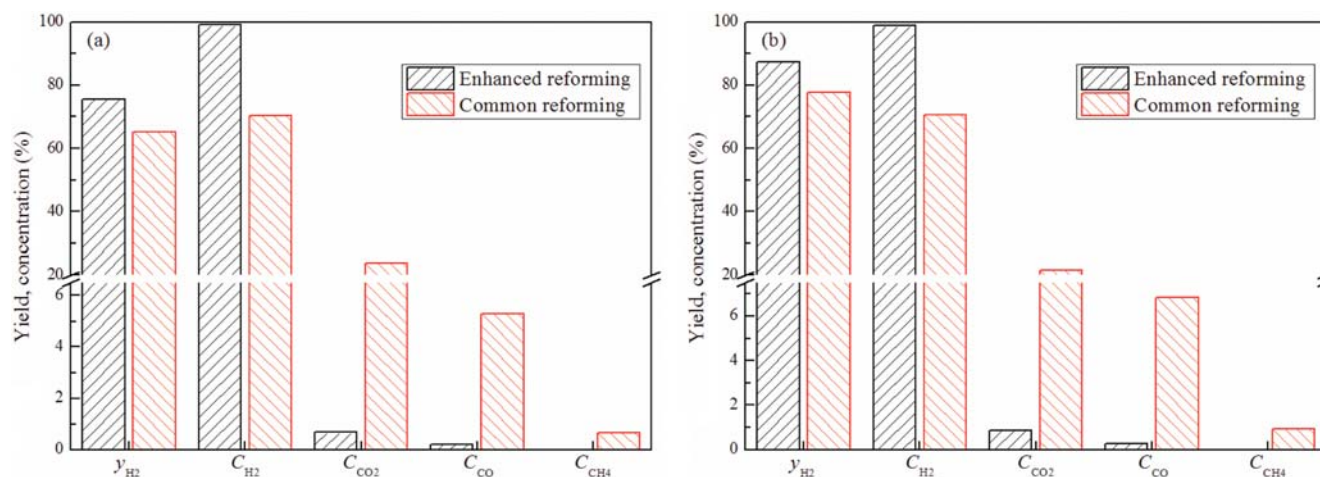


Fig. 7. Results of the reforming experiments. (a) at 700 °C and (b) at 800 °C.

Table 2. The comparison of the experimental and thermodynamic values

Temperature	Type	Enhanced reforming (%)					Common reforming (%)				
		y_{H_2}	C_{H_2}	C_{CO_2}	C_{CO}	C_{CH_4}	y_{H_2}	C_{H_2}	C_{CO_2}	C_{CO}	C_{CH_4}
700 °C	Experimental	75.55	99.10	0.68	0.22	0	65.24	70.32	23.88	5.30	0.67
	Thermodynamic	98.31	89.04	9.50	1.46	0	94.81	69.94	26.23	3.82	0
800 °C	Experimental	87.35	98.85	0.88	0.27	0	77.72	70.65	21.70	6.84	0.93
	Thermodynamic	94.83	76.78	19.07	4.15	0	92.89	69.51	25.17	5.32	0

directions of H₂ production, with very low concentrations of CH₄ and CO and a fairly high H₂ concentration at the initial stage. The above results indicated the sorption-enhanced SR reaction occurring, so this stage was named the “enhanced reforming stage” in this paper. However, as time passed, the CO₂ adsorption amount of the sorbent packed in the SR reactor tended to saturation, with the increases of carbon-containing gas (CO₂, CO and CH₄) concentration and the decrease of H₂ concentration. Then, the reaction process regained stability, with the H₂ concentration of about 70% and the CO₂ concentration between 20% and 25%. Such a composition distribution in the reformed gas was similar to that with no addition of any CO₂ sorbent [9], so this stage was named “common reforming stage” in this paper.



The reforming results (average values) at the two stages were compared, shown in Fig. 7. From the figure, both of the (average) H₂ yield and concentration in the enhanced reforming stage were obviously higher than both of those in the common reforming stage, indicating that the added CO₂ sorbent played an important role. In the common reforming stage, due to high temperature accelerating endothermic reforming reactions, the H₂ yields were 65.24% at 700 °C and 77.72% at 800 °C, yet with both of the H₂ concentrations about 70%. But the exothermic WGS reaction was to some extent inhibited at high temperature, causing the slightly higher CO concentration at 800 °C. However, the addition of CO₂ sorbent

changed the reforming process. In the enhanced reforming stage, due to the reforming reaction accelerated, more H₂ was produced with the yields being 75.55% at 700 °C and 87.35% at 800 °C. The H₂ concentration was improved most obviously, reaching over 98.85%, and the content of the carbon-containing gases was very low, with no CH₄.

Then, the experimental results were compared with the thermodynamic results, shown in Table 2. The thermodynamic analysis of the tar steam reforming process was performed based on the Gibbs free energy minimization, stating as isothermal conditions with heat loss ignored and regardless of the kinetics. In the SESR analysis, CaO was selected as the CO₂ sorbent, with the CaO/C ratio (the mole ratio of the CaO and the carbon in the bio-oil) set as 2 : 1. For the common reforming, the compositions of the reformed gases experimental and thermodynamic were similar, but the H₂ yields had greater differences, because the mass and heat transfer in the reactor, the used catalyst activity and stability including whether the aggregation or the carbon deposition occurred in a long-running process, limited the steam reforming reaction course in the real experiment, while these factors were ignored in the thermodynamic analysis. For the enhanced reforming, there were still much greater differences between the experimental and thermodynamic compositions of the reformed gases as well as the H₂ yields, but the gaps between H₂ yields was diminished.

For the enhanced reforming via thermodynamic analysis, all the carbon in the reaction system was almost converted into CaCO₃ before 600 °C (seen in Fig. 8), indicating that the sorption-enhanced steam reforming of tar went on very thoroughly and the obtained

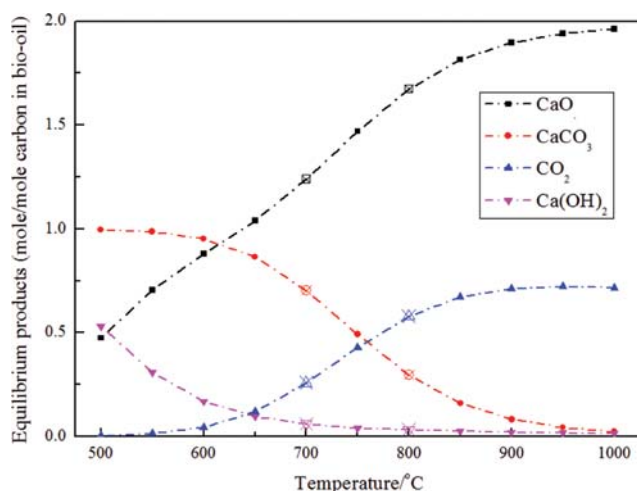


Fig. 8. Equilibrium products involved in the reactions related with CaO.

H₂ yield and concentration approached 100%. But, after 600 °C, the H₂ yield and concentration obtained from thermodynamic analysis decreased with the temperature increasing (seen in Table 2). For one thing, the exothermic WGS reaction was one of the main controlling links in the tar steam reforming process, thus causing the H₂ decrease with the CO increase. For another, the CO₂ adsorption capacity of CaO declined thermodynamic when the temperature went over about 600 °C (seen in Fig. 8), attributed to the endothermic adsorption reaction (Eq. (6)), and therefore, the CO₂ concentration increased with the H₂ decrease. However, from the experimental results, the H₂ yield was improved when the temperature increased from 700 °C to 800 °C, mainly because in a certain temperature scope the activation energy of the reforming reactions and the activity of the reforming catalyst were improved as the temperature rose. Compared to the thermodynamic results, the CO₂ concentrations from the reforming experiments were obviously lower, with obviously higher H₂ concentrations. It was mainly attributed to the fact that the best temperatures of realistic CaO based sorbents to adsorb CO₂ were commonly between 700 °C and 800 °C, which were obviously higher than the best thermodynamic temperature [15,19,34].



CONCLUSIONS

CO₂ sorbents with Ca₁₂Al₁₄O₃₃ as carrier were prepared under five different methods: solid-states-reaction method (SSR), co-precipitation (CP) method, solid-liquid mixing (SLM) method, sol-gel (SG) method and impregnation (IM) method. From the characterization, among all the samples prepared by these five methods, the samples with SG and IM showed obvious characteristic peaks of CaO and Ca₁₂Al₁₄O₃₃ and no interference phases in XRD patterns. But, compared to IM, the sample with SG had much smaller-size grains distributed evenly on the sorbent surface and better pore structure. The characterization results provided powerful support for the CO₂ adsorption performances of all the samples,

with the sample prepared with SG showing the best CO₂ adsorption capacity and excellent long-term cyclic stability. Then, the sorbent was used into the reforming experiments of 1-methylnaphthalene (C₁₁H₁₀) as the tar model component. Under the action of the sorbent, the reforming reaction was enhanced in-situ, with the H₂ yield and concentration improved obviously. Especially for H₂ concentration, it can reach 98.85% above. And, at 800 °C, the H₂ yield from the enhanced reforming can reach 87.35%, approaching the thermodynamic value.

ACKNOWLEDGEMENTS

This research was financially supported by the National Natural Science Foundation of China (51604077), Major State Research Development Program of China (2017YFB0603603), the Fundamental Research Funds for the Central Universities (N172504019) and the Doctoral Scientific Research Foundation of Liaoning Province (201601004).

REFERENCES

1. N. B. Gao, S. Liu, Y. Han, C. Xing and A. M. Li, *Int. J. Hydrogen Energy*, **40**, 7983 (2015).
2. C. P. B. Quitete, R. C. P. Bittencourt and M. M. V. M. Souza, *Appl. Catal. A-Gen.*, **478**, 234 (2014).
3. J. Yang, X. Wang, L. Li, K. Shen, X. Lu and W. Ding, *Appl. Catal. B Environ.*, **96**, 232 (2010).
4. H. Q. Xie, Q. B. Yu, J. R. Zhang, J. L. Liu, Z. L. Zuo, J. L. Liu and Q. Qin, *Environ. Prog. Sust. Energy*, **36**, 729 (2017).
5. H. Q. Xie, Q. B. Yu, Z. L. Zuo, J. R. Zhang, Z. C. Han and Q. Qin, *J. Therm. Anal. Calorim.*, **126**, 1621 (2016).
6. B. Yue, X. Wang, X. Ai, J. Yang, L. Li, X. Lu and W. Ding, *Fuel Process. Technol.*, **91**, 1098 (2010).
7. J. L. Colby, T. Wang and L. D. Schmidt, *Energy Fuels*, **24**, 1341 (2010).
8. R. Zhang, Y. Wang and R. C. Brown, *Energy Convers. Manage.*, **48**, 68 (2007).
9. H. Q. Xie, J. R. Zhang, Q. B. Yu, Z. L. Zuo, J. L. Liu and Q. Qin, *Energy Fuels*, **30**, 2336 (2016).
10. C. Li, D. Hirabayashi and K. Suzuki, *Fuel Process. Technol.*, **90**, 790 (2009).
11. T. Furusawa and A. Tsutsumi, *Appl. Catal. A-Gen.*, **278**, 195 (2005).
12. D. Swierczynski, C. Courson and A. Kiennemann, *Chem. Eng. Process.: Process Intensif.*, **47**, 508 (2008).
13. W. B. Widayatno, G. Guan, J. Rizkiana, X. Hao, Z. Wang, C. Samart and A. Abudula, *Fuel*, **132**, 204 (2014).
14. J. Yang, X. G. Wang, L. Li, K. Shen, X. G. Lu and W. Z. Ding, *Chem. J. Chinese Univ.*, **31**, 1841 (2010).
15. H. Q. Xie, Q. B. Yu, Z. L. Zuo, Z. C. Han, X. Yao and Q. Qin, *Int. J. Hydrogen Energy*, **41**, 2345 (2016).
16. Z. Yang, Y. Zhang, W. Ding, Y. Zhang, P. Shen, Y. Zhou, Y. Liu, S. Huang and X. Lu, *J. Nat. Gas Chem.*, **18**, 407 (2009).
17. H. Q. Xie, Q. B. Yu, X. Yao, W. J. Duan, Z. L. Zuo and Q. Qin, *J. Energy Chem.*, **24**, 299 (2015).
18. C. Li, D. Hirabayashi and K. Suzuki, *Appl. Catal. B Environ.*, **88**, 351 (2009).

19. B. L. Dou, C. Wang, Y. C. Song, H. S. Chen, B. Jiang, M. J. Yang and Y. J. Xu, *Renew. Sust. Energy Rev.*, **53**, 536 (2016).
20. A. L. Ortiz and D. P. Harrison, *Ind. Eng. Chem. Res.*, **40**, 5102 (2001).
21. C. S. Martavaltzi and A. A. Lemonidou, *Micropor. Mesopor. Mater.*, **110**, 119 (2008).
22. C. M. Kinoshita and S. Q. Turn, *Int. J. Hydrogen Energy*, **28**, 1065 (2003).
23. H. Q. Xie, Q. B. Yu, M. Q. Wei, W. J. Duan, X. Yao, Q. Qin and Z. L. Zuo, *Int. J. Hydrogen Energy*, **40**, 142 (2015).
24. H. Q. Xie, Q. B. Yu, H. Lu, Y. Y. Zhang, J. R. Zhang and Q. Qin, *Int. J. Hydrogen Energy*, **42**, 28718 (2017).
25. I. Zamboni, C. Courson and A. Kiennemann, *Catal. Today*, **176**, 197 (2011).
26. J. Blamey, E. J. Anthony, J. Wang and P. S. Fennell, *Prog. Energy Combust. Sci.*, **36**, 260 (2010).
27. M. M. Xie, Z. M. Zhou, Y. Qi, Z. M. Cheng and W. K. Yuan, *Chem. Eng. J.*, **207-208**, 142 (2012).
28. Z. M. Zhou, Y. Qi, M. M. Xie, Z. M. Cheng and W. K. Yuan, *Chem. Eng. Sci.*, **74**, 172 (2012).
29. C. S. Martavaltzi and A. A. Lemonidou, *Ind. Eng. Chem. Res.*, **47**, 9537 (2008).
30. E. C. Vagia and A. A. Lemonidou, *Appl. Catal. A: Gen.*, **351**, 111 (2008).
31. F. Chen, Y. R. Hong, J. L. Sun and J. L. Bu, *J. Univ. Sci. Technol. Beijing*, **13**, 82 (2006).
32. Z. S. Li, N. S. Cai, Y. Y. Huang and H. J. Han, *Energy Fuels*, **9**, 1447 (2005).
33. L. Gong, Z. Lin, S. Ning, J. Sun, J. Shen, Y. Torimoto and Q. Li, *Mater. Lett.*, **64**, 1322 (2010).
34. I. Zamboni, C. Courson and A. Kiennemann, *Catal. Today*, **176**, 197 (2011).